DOI: 10.2478/fas-2023-0007
FATIGUE OF AIRCRAFT STRUCTURES
Volume 2023: Issue 15, pp. 115–132

A COMPARISON OF FREE AND MAPPED MESHES FOR STATIC STRUCTURAL ANALYSIS

Aun Haider
Institute of Aeronautics and Avionics, Air University Islamabad,
E-9/4 E-9, Islamabad, Islamabad Capital Territory 44000, Pakistan.

aunbutta@gmail.com

Abstract

This study addresses the challenge faced by Finite Element Analysts when choosing between free and mapped meshes, especially in terms of convergence stability and solution accuracy. The investigation focuses on 3D solid models under static structural loading, analyzed using Ansys® and MSC Patran®. Both free and mapped mesh types, employing equivalent 3D solid elements, are used to assess an aircraft structural component under design load conditions, with fixed boundaries. For free meshes, Tet10 elements in Patran (equivalent to Solid 72 in Ansys) are used, whereas for mapped meshes, CPENTA / CHEXA elements in Patran (equivalent to Wed6 / Hex8 in Ansys) are employed. Mesh convergence studies ensure that discretization does not affect the numerical solution. Notably, a significant stress increase is observed with successive refinement of free meshes, while mapped meshes achieve mesh independence at coarser refinement levels. Comparison of fringe plots indicates the same location for maximum deformation and equivalent stress in both free and mapped mesh models. The findings demonstrate that free meshes tend to underpredict maximum deformation and equivalent stress compared to mapped meshes, with both meshes showing deformation and stress at consistent locations. The findings underscore the importance of carefully choosing the appropriate mesh type, particularly when analyzing critical structural components, to ensure reliability and accuracy in FEA simulations.

Keywords: mesh convergence, mesh independence, discretization scheme, Finite Element Analysis, FE Software.
Article category: research article

Introduction

Finite Element Analysis (FEA) is a numerical method used to provide approximate solutions for problems that lack closed-form analytical solutions (Kurowski, 2022). The core principle of Finite Element Modelling (FEM) involves creating a mathematical representation that closely mimics the geometry of real-world structures, generating responses that are deemed equivalent when appropriate modeling techniques are applied (Hoppe, 2023). In essence, FEA enables detailed analysis of complex engineering and physical systems by discretizing them into smaller elements. The accuracy of the results depends on the fidelity of the mathematical model with respect to the physical reality, and on the careful application of numerical techniques throughout the simulation process.

Discretization of the problem domain involves generating a mesh model, which serves as a bridge between the computer aided design (CAD) model and the Finite Element (FE) solver. When the mesh is submitted to the FE solver, it is inherently assumed to accurately represent the component's geometry. Therefore, the quality of the mesh plays a pivotal role in determining the accuracy of solution (Schröder et al., 2021).

Two distinct types of meshing strategies are commonly employed: the "free mesh," also known as an unstructured mesh, and the "mapped mesh," also referred to as a structured or regular mesh. A free mesh forgoes the constraints of a predefined pattern or grid structure, allowing for irregular arrangement of mesh element – typically triangles in 2D, or tetrahedra in 3D. This flexibility proves invaluable when modeling intricate geometries, where imposing a structured mesh might prove impractical. A mapped mesh, on the other hand, employs a structured pattern, akin to a grid. This mesh type predominantly relies on quadrilateral and hexahedral elements for 2D and 3D bodies, respectively (Papadimitrakis et al., 2022). The mapped mesh's structured nature offers simplicity in both generation and manipulation, particularly in applications where the geometry exhibits well-behaved characteristics and can be effectively represented by a structured grid (Pietroni et al., 2022).

In physics simulations, the choice between free and mapped meshes hinges on the specific nature of the problem at hand. Factors such as computational efficiency, accuracy requirements, the geometry of the problem, and the nature of the physical system being simulated play pivotal roles in this decision-making process (Sher et al., 2020). Neither meshing technique is inherently superior; each has its own strengths and weaknesses, contingent upon such factors as the geometric intricacies of the problem, the underlying physics, and the targeted level of precision (Liu et al., 2021).

A free mesh, with its flexibility and adaptability to complex, dynamic, more deformable geometries, is particularly advantageous in simulations involving complex shapes. A mapped mesh, in contrast, characterized by adherence to the geometry of the simulation domain, is resource-efficient and well-suited for scenarios featuring stable and well-defined geometries, such as structural analyses. In many cases, a hybrid meshing approach can be judiciously employed to strategically exploit the strengths of both free and mapped meshes across different sections of the simulation domain. This hybrid approach becomes particularly relevant when dealing with multifaceted simulation domains exhibiting varying geometric characteristics (Jiang et al., 2021).

Engineers and researchers typically undertake mesh sensitivity analyses to assess how meshing choices affect both simulation outcomes and computational efficiency, iteratively refining the mesh to optimize its efficacy for the specific problem at hand. Stress analysts, for instance, commonly rely on the automatic mesh generators integrated into commercial software platforms, owing to the inherent convenience they offer in the meshing process (Smitha 2021). Nevertheless, the decision to opt for either free or mapped mesh types, particularly in conjunction with the automatic mesh generators found in Finite Element Analysis (FEA) software such as Ansys® and MSC Patran®, requires careful consideration on the part of the analyst (Okereke et al., 2018).

Ansys and MSC Patran are prominent FEA software solutions, each offering a suite of tools that include numerous checks to ensure the creation of a sound mesh model. Note, however, that while these software packages provide safeguards against a poor mesh, they do not inherently prevent analysts from inaccurately representing the problem domain (Ereiz et al., 2022). Thus, the responsibility ultimately rests with the analyst to exercise due diligence in making informed decisions regarding meshing strategies and ensuring a faithful representation of simulation domain (Park et al., 2019).

This growing inclination among Finite Element (FE) analysts to prefer free meshes over mapped meshes is primarily fueled by a belief or assumption that both types of meshes will produce comparable results, as long as proper mesh convergence is attained (Marcé-Nogué et al., 2020). This belief has led to the unfortunate misconception that the choice between using a free or mapped mesh is a noncritical factor in Finite Element (FE) analysis, erroneously implying that free and mapped meshes have a negligible influence on the accuracy of FE results, once mesh convergence is achieved (Ruggiero et al., 2019).

While achieving mesh convergence is undoubtedly critical for ensuring solution accuracy, the selection between free and mapped meshes nevertheless involves more nuanced considerations (Jalammanavar et al., 2018) The geometry of the problem, the nature of the physics involved, and the specific requirements of the simulation can significantly impact the appropriateness of one mesh type over the other.

While certain convenient benchmarks for mesh convergence have been established (De Mooij et al., 2019), a notable gap exists in literature in terms of comprehensive comparisons between free meshes utilizing tetrahedral elements and mapped meshes employing wedge/hexahedral elements in a broader context. Additionally, there appears to have been insufficient reviews regarding the impact of the automatic mesh generators available in Finite Element Analysis (FEA) software (İrsel, 2019). The absence of a comparative analysis between free meshes with tetrahedral elements and mapped meshes with wedge/hexahedral elements suggests a potential gap in understanding the performance of these meshing strategies across diverse simulation scenarios. Such a comparison is nevertheless crucial for discerning the strengths and limitations of each approach in different problem domains and could contribute valuable insights into optimizing mesh selection based on specific requirements. Furthermore, the influence of automatic mesh generators in FEA software underscores the need for a comprehensive examination of their efficacy in producing accurate and reliable meshes. Investigating the comparative performance of different automatic mesh generators could also enhance the overall reliability and accuracy of numerical simulations.

The primary aim of this study, therefore, is to assess and compare the performance of structured/mapped mesh and unstructured/free mesh in the context of static structural analysis for a solid model using two prominent Finite Element Analysis (FEA) software tools, namely Ansys and Patran.

The study involves conducting Finite Element (FE) Analysis on a three-dimensional solid model representing a structural component of an aircraft wing. The analysis begins by assigning appropriate material properties to the CAD model. The problem domain is then discretized using both free and mapped meshes, in both Ansys and Patran. A static structural analysis of the component then is carried out under specific design load conditions, with fixed boundary conditions. The analysis focuses on evaluating equivalent stress results generated using the different FE models with both mesh types. A thorough comparison of the equivalent stress results obtained from these diverse FE models is then carried out.

This research aims to provide meaningful insights and formulate guidelines for selecting the appropriate mesh type when performing static structural analysis of components subjected to design loads. By systematically comparing the performance of structured/mapped mesh and unstructured/free mesh in the specific context of Ansys and Patran, this study aims to provide valuable recommendations and guidelines that can aid engineers and analysts in making informed decisions regarding mesh selection for similar structural analyses.

Methodology

Static structural analysis of an aircraft wing's structural member, the wing tulip, was carried out using two prominent FE software tools: Ansys and MSC Patran. The CAD model was generated using SpaceClaim Design Modeller®, with the material properties assigned as linear elastic and isotropic.

Meshing was performed in Ansys and MSC Patran, generating both free and mapped meshes. Tetrahedral elements were utilized for the free mesh, while wedge and hexahedral elements are employed for the mapped mesh (Sabat & Kundu, 2020). Both types of elements employed featured quadratic shape functions, meaning nodes were positioned at the corners and mid-sides of the element, allowing for a parabolic approximation of the solution. Quadratic elements can capture more complex variations in the solution field and typically offer higher accuracy than linear elements, albeit at a higher computational cost.

A fixed boundary condition, constraining all 6 degrees of freedom, was applied at the attachment bolt holes. Utilizing the default solver settings, a static structural analysis of the wing tulip was carried out under the design load. Successive mesh refinements were carried out until discretization errors reached acceptable limits (Arndt et al., 2021). A grid-independent solution was considered to be achieved when the percent change in equivalent stress between two successive mesh refinements was less than 5% (Nemade & Shikalgar 2020).

Maximum deformation results were also analyzed, where deformation refers specifically to the relative displacement of points within the structure, excluding rigid body translations. Finally, the study finally compared the results from both free and mapped mesh models to identify any significant differences.

Results

CAD Model of Component

CAD model of the component was developed in SpaceClaim Design Modeler®. Figure 1 shows the CAD model, which is imported in IGES format to both MSC Patran and Ansys®. Using this CAD model as a template, both free (unstructured) and mapped (structured) mesh is generated in each software package. The component was made of alloy 30CrMnSiA, which has a modulus of elasticity (E) of 196 GPa, a yield strength (σ_y) of 835 MPa, and a Poisson ratio (μ) of 0.3.

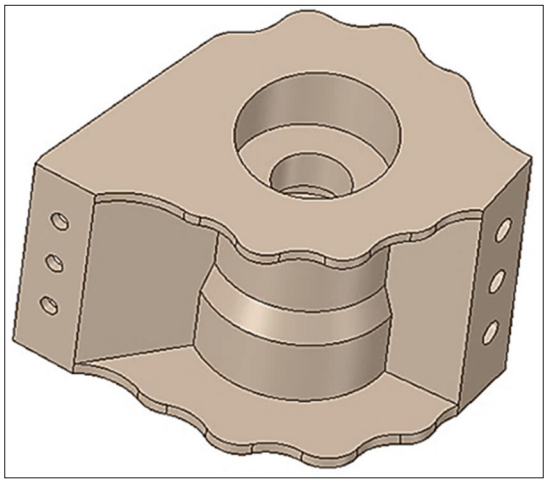

Fig. 1. CAD Model of Component.

Loads on Component

Table 1 outlines the design loads applied to the component, specified as force and moment vectors. Finite element analysis were conducted under these design load conditions using both free and mapped meshes in Patran and Ansys.

Table 1. Design loads for model

Force	Magnitude (N)	Moment	Magnitude (Nm)
Fx	30,100	*Mx*	718
Fy	9,510	*My*	36.8
Fz	37,300	*Mz*	1.0

FEA with Free Mesh in Patran

The CAD model was imported into Patran in IGES format. MSC Patran, serving as a pre / post processing tool for the FE Solver Nastran®, was used to apply loads and boundary condition as shown in Figure 2. The solid CAD model was meshed using Tet10 3D solid elements – tetrahedral elements with 10 nodes – to create the free mesh. Midside nodes on each element side are present to ensure quadratic shape functions. Patran affords the analyst flexibility in varying the global mesh density. A mesh convergence study was carried out to establish a numerical model independent of mesh density.

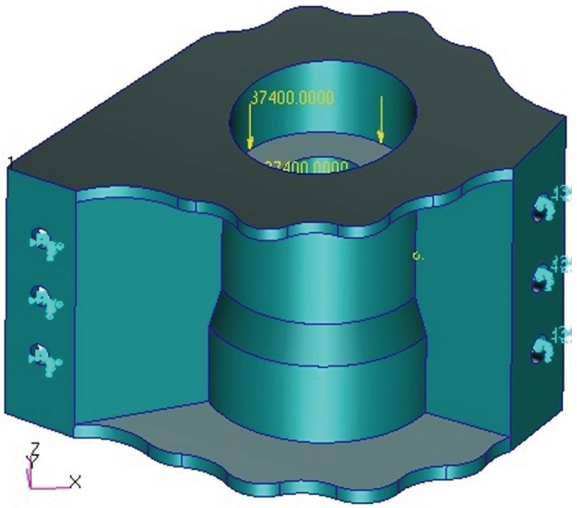

Fig. 2. Loads and Constraints for Free Mesh in Patran.

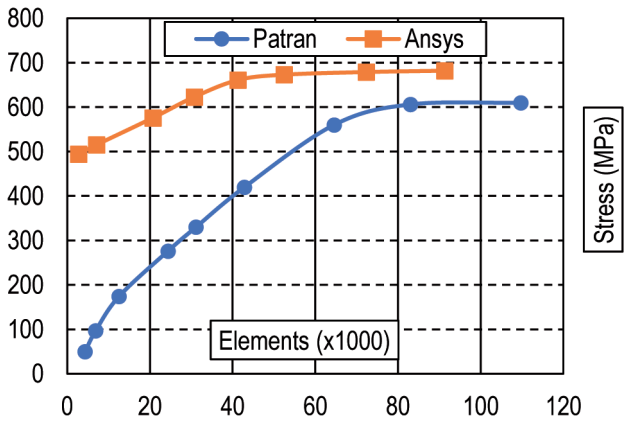

Fig. 3. Free Mesh Convergence Study.

Figure 3 illustrates that the maximum stress value became independent of mesh density at 82,998 elements. A further increase in number of elements did not change the magnitude of equivalent stress.

The free mesh model is shown in Figure 4. After the FE model was developed in Patran, it was submitted to the solver. Post processing of the solution file provides deformation and stress fringe plots.

Deformation field of model under the applied load is displayed in Figure 5. A maximum deformation of 0.287 mm is observed at the point of interest, i.e., the flange of the model. Note that in this context, deformation refers specifically to the relative movement of points within the structure, excluding rigid body translations. Furthermore, the model is fully constrained to prevent any rigid body motion.

The stress field of the model under the applied load is given in Figure 6. Maximum stress (606 MPa) is observed at the bolt hole. Based on the material's yield strength, the calculated Factor of Safety (FOS) for the free mesh in Patran is 1.38.

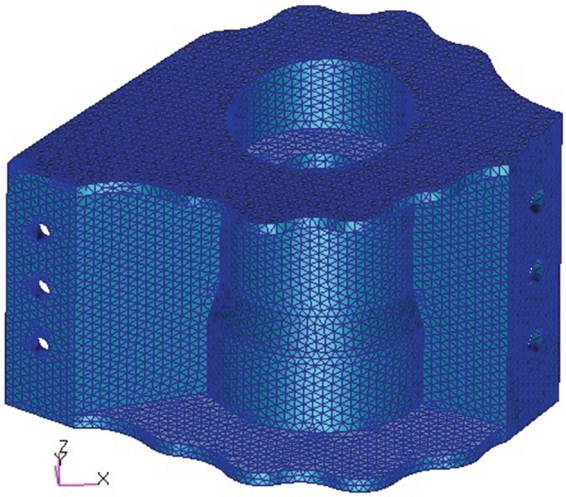

Fig. 4. Free Mesh in Patran.

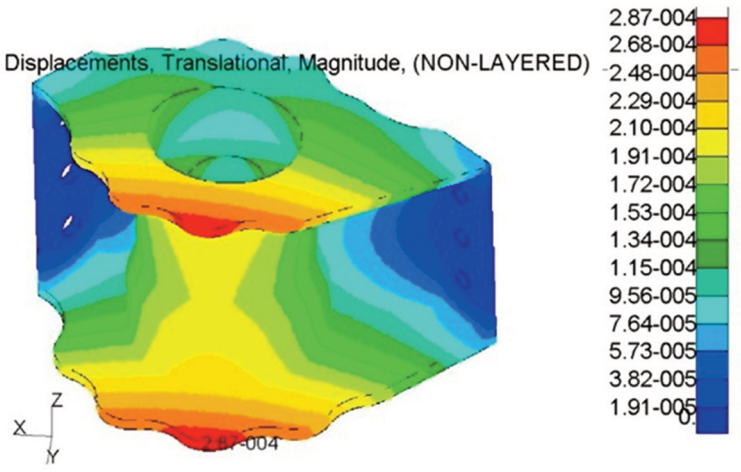

Fig. 5. Deformation with Free Mesh in Patran.

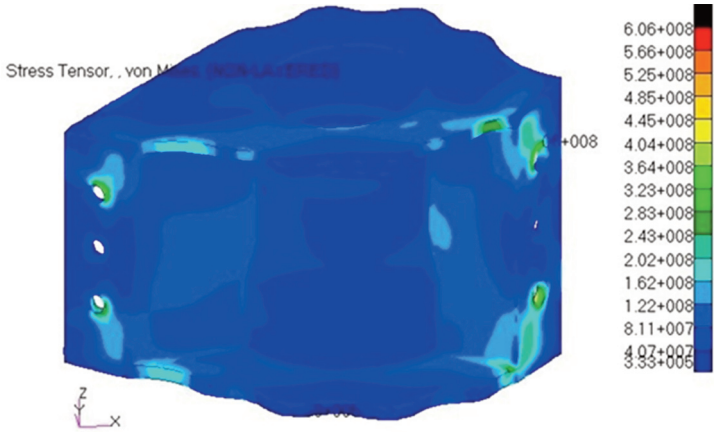

Fig. 6. Stress with Free Mesh in Patran.

FEA with Free Mesh in Ansys

The CAD model of the component was also imported into Ansys in the IGES format. Figure 7 shows the applied loads and boundary condition for the Ansys model. A similar mesh convergence study was performed to generate an FE model with stress field independent of mesh density. Figure 3 shows that the solution becomes independent of mesh size at 72,321 elements.

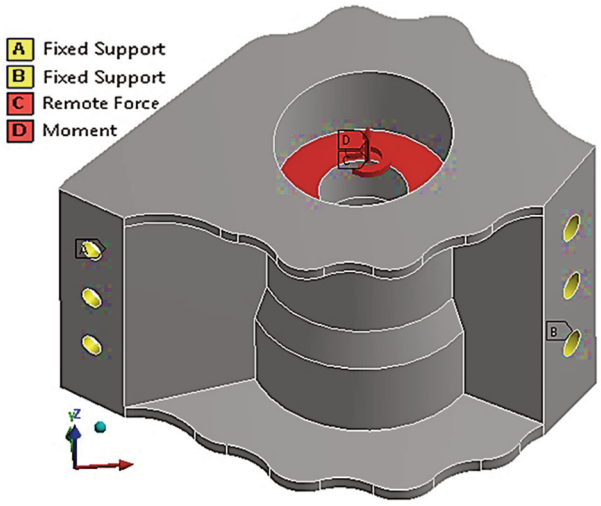

Fig. 7. Loads and Constraints for Free Mesh in Ansys.

Tetrahedral elements (Solid72) with midside nodes were used for meshing in Ansys. The presence of midside nodes provides a quadratic shape function, improving the interpolation of deformation values between the corners. To accurately capture stress gradients, local mesh refinement was carried out at areas of stress concentration and geometric transition.

Figure 8 shows the free mesh model in Ansys. The deformation field of the model under the applied loads is given in Figure 9, with the maximum deformation of 0.13 mm observed at the flange of the model.

The equivalent stress on the model under the design load is given in Figure 10. Maximum stress 674 MPa is observed at the bolt holes of the model. Based on the material's yield strength, the Factor of Safety was calculated to be 1.24.

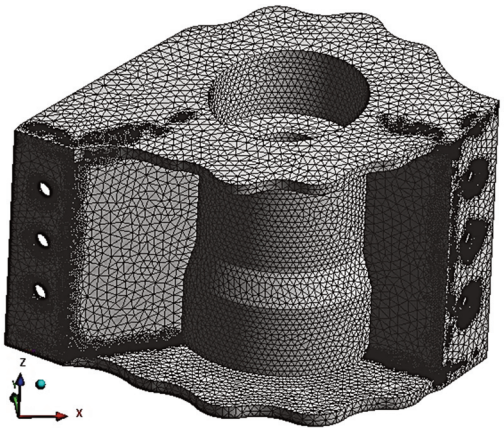

Fig. 8. Free Mesh in Ansys.

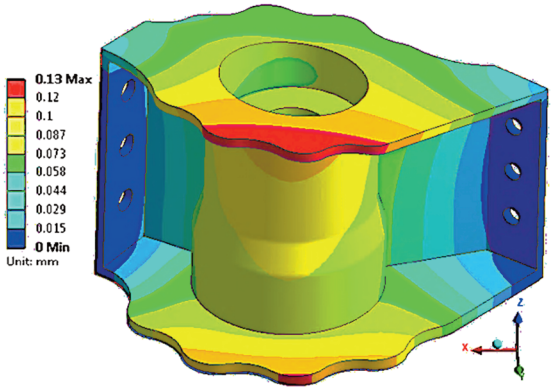

Fig. 9. Deformation with Free Mesh in Ansys.

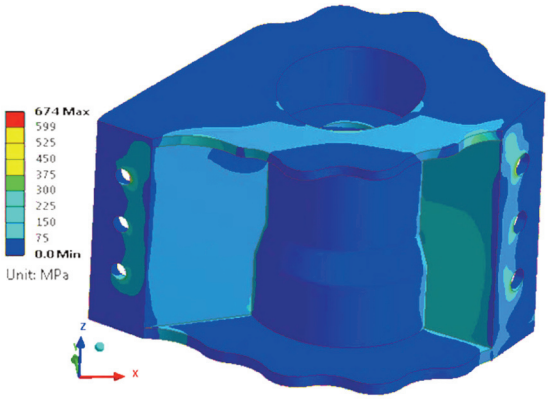

Fig. 10. Stress with Free Mesh in Ansys.

FEA with Mapped Mesh in Patran

A mapped mesh for the model was generated in MSC Patran for the Nastran solver, using wedge-shaped (CPENTA) and brick-shaped (CHEXA) solid elements. Both CPENTA and CHEXA elements are quadratic, containing midside nodes—CPENTA elements have 15 nodes, while CHEXA elements have 20 nodes. These elements preserve six degrees of freedom (DOFs) at each node, allowing for more accurate representation of complex stress and strain distributions within the structure.

RBE2 multipoint constraints (MPC 184) were applied at the bolt holes of the model, effectively constraining both translation and rotation in these areas. Figure 11 illustrates the mapped mesh and applied constraints on the model.

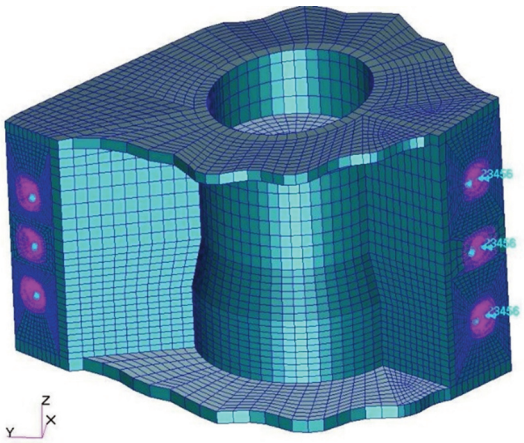

Fig. 11. Constraints on FE Model in Patran.

Figure 12 shows the applied design load applied as equivalent nodal forces on the finite elements of the model. A mesh convergence study was carried out for the mapped mesh. Figure 13 shows that the solution became independent of mesh density at 7,481 elements.

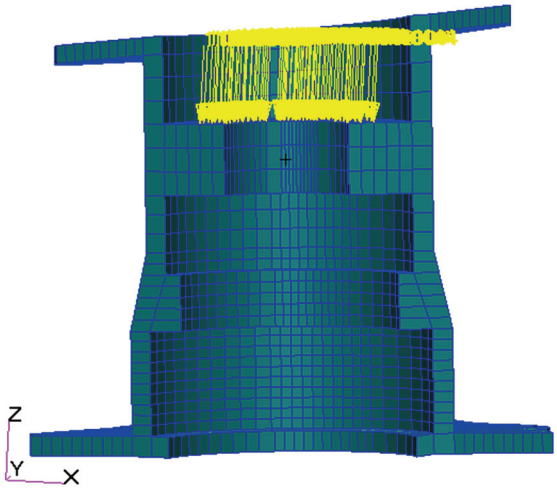

Fig. 12. Loads on Mapped Mesh in Patran.

Once the finite element analysis was performed in Nastran, the solution file was post-processed in Patran to obtain fringe plots for deformation and stress. The deformation field of the model under the applied load is given in Figure 14. Maximum deformation of 0.275 mm was observed at the flange of the model.

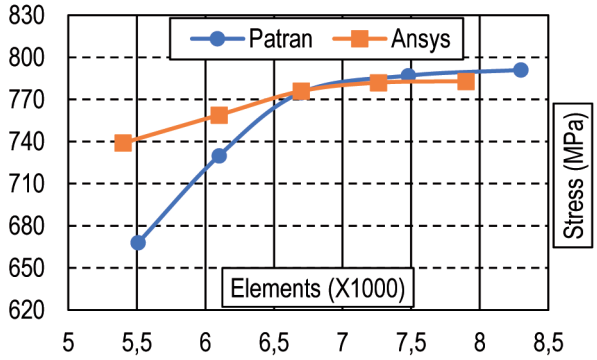

Fig. 13. Mapped Mesh Convergence Study.

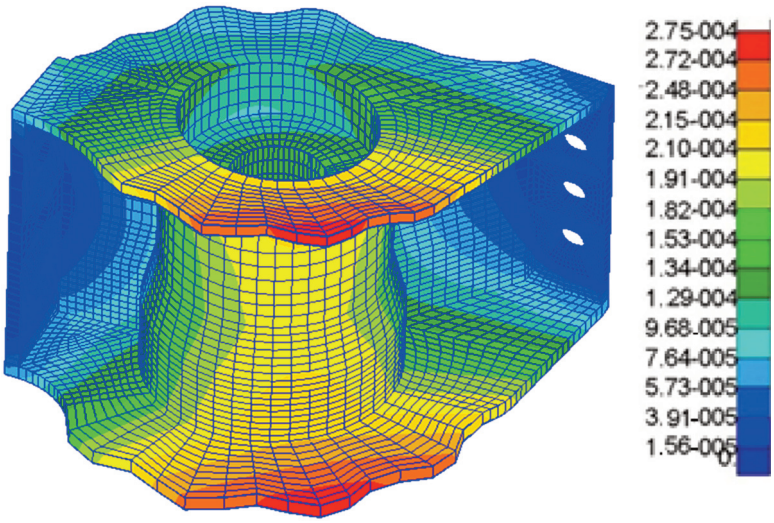

Fig. 14. Deformation for Mapped Mesh in Patran.

Equivalent stress field of the model is given in Figure 15, with maximum stress of 787 MPa observed at bolt hole of the model. Based on the material's yield strength, the Factor of Safety (FOS) for the mapped mesh in Patran was calculated to be 1.06.

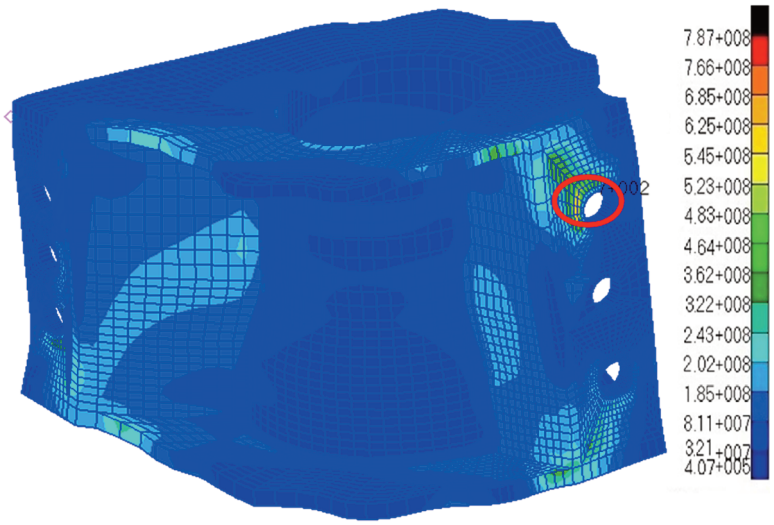

Fig. 15. Stress for Mapped Mesh in Patran.

FEA with mapped mesh in Ansys

The CAD model was imported into Ansys, where mapped meshing was applied using edge and element sizing. Figure 16 shows the applied loads and boundary conditions on the model. The mapped mesh convergence study, shown in Figure 13, identifies that the solution becomes independent of mesh size at 7,264 elements.

Wed6 and Hex8 Solid 182 elements are used for meshing the model. Both elements have midside nodes to enforce quadratic shape functions. The mapped mesh generated in Ansys is shown in Figure 17.

FE analysis of the model was carried out under the applied load and boundary conditions. The deformation field for the model the applied load is given in Figure 18, with a maximum deformation of 0.32 mm observed at the flange of the model.

The stress field on the model under the applied load is shown in Figure 19, with the m aximum equivalent stress of 782 MPa observed at the bolt holes of the model.

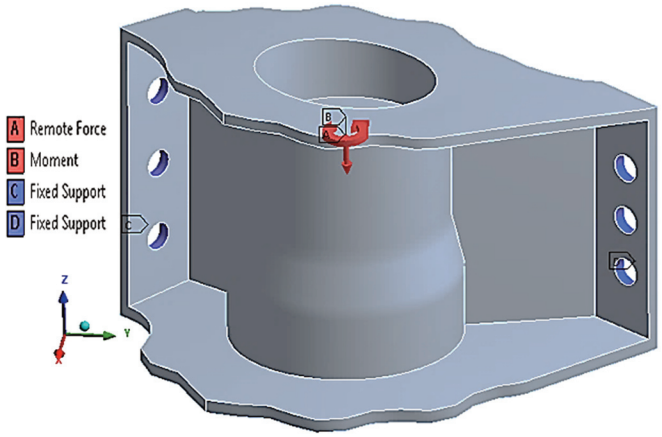

Fig. 16. Loads and Constraints for Mapped Mesh in Ansys.

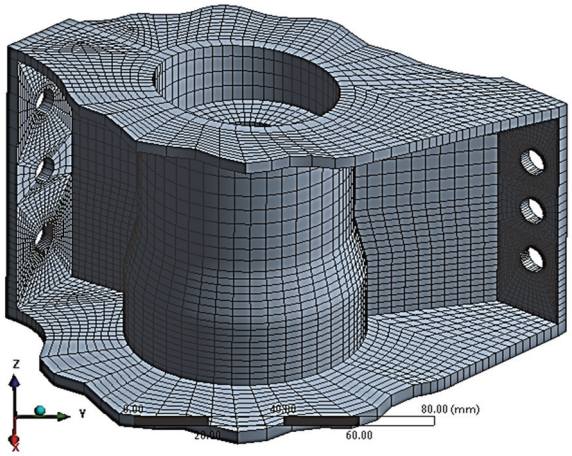

Fig. 17. Mapped Mesh in Ansys.

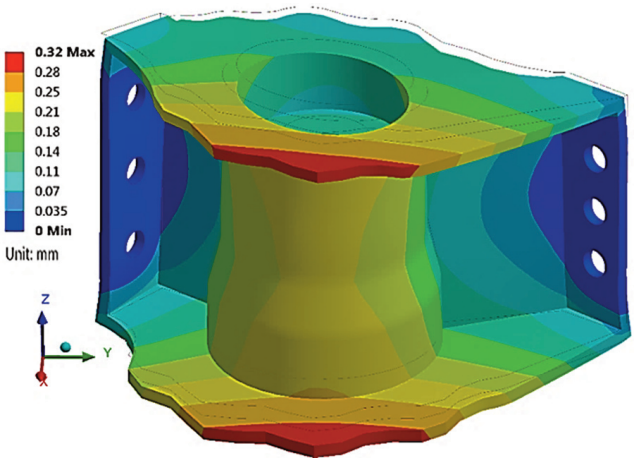

Fig. 18. Deformation with Mapped Mesh in Ansys.

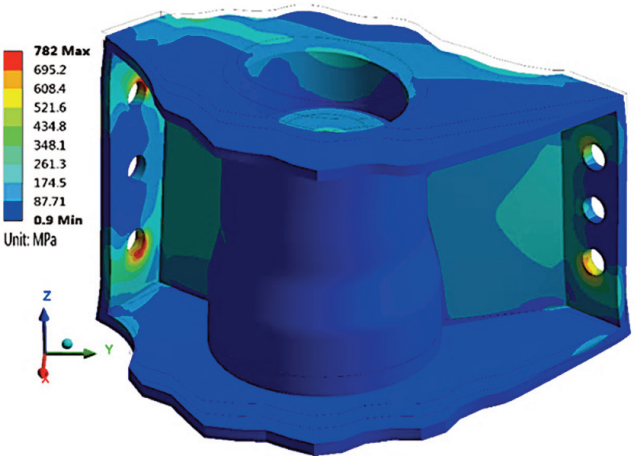

Fig. 19. Stress with Mapped Mesh in Ansys.

Discussion

This study examined the performance of free meshes based on quadratic tetrahedral elements versus mapped meshes based on quadratic wedge / hexahedral elements, generated in two FEA software tools: Ansys and MSC Patran. Comparing the FE results from these two leading tools was performed to verify the preferences of FE analysts for particular software based on meshing performance and simulation accuracy (Magomedov and Sebaeva 2020).

Both free and mapped meshes were used for static structural analysis of a wing tulip component under the design load. Table 2 summarizes the key differences and similarities between the free and mapped mesh models across both software platforms. Equivalent mesh elements were used in each case: the solid Tet10 element in Patran corresponds to the Tetrahedral (Solid 72) element in Ansys, while CPENTA / CHEXA elements in Patran are equivalent to Wed6 / Hex8 (Solid 182) elements in Ansys, respectively. Both element types preserve midside nodes to enforce a quadratic shape function. A mesh convergence study was carried out to determine appropriate mesh with no effect of discretization on the solution.

Free mesh generation from the CAD model was straightforward in both FEA software platforms. However, in Patran, mesh elements and global mesh density parameters can only be adjusted globally, without the option for local mesh refinement at areas of interest, such as stress concentration zones. In contrast, Ansys provides full control over meshing parameters, including element type, shape function, mesh density, and the ability to refine local and global mesh densities.

Table 2. Comparison of Free and Mapped Mesh in Patran and Ansys.

Quantity	Patran Mesh		Ansys Mesh	
	Free	Mapped	Free	Mapped
Element Type	Tet10	CPENTA/CHEXA	Solid72	Solid182
Element Shape	Tetra	Wedge/Brick	Tetra	Wedge/Brick
Nodes per Element	10	15/20	10	15/20
Shape Function	Quadratic			
Total Elements	82998	7481	72321	7264
Deformation (mm)	0.287	0.275	0.13	0.32
Stress (MPa)	606	787	674	782
FOS	1.38	1.06	1.24	1.07

Generating the mapped mesh required considerable time and effort from the analyst in both software tools. In particular, edge and element sizing had to be creatively managed, especially at transition zones between wedge and hexahedral elements.

Comparing the deformation and stress fringe plots for different meshes in both FEA software platforms reveals that all mesh models consistently identified the same location of maximum deformation and maximum equivalent stress. The maximum deformation was observed at the flange of the model and the maximum stress at the location of the bolt holes. Contrary to the work of Shah et al. (2022), therefore, this study identified same stress hot spots in both commercially available software

In Patran, the maximum stress observed was 49.6 MPa for the free mesh of 4,295 elements. As the mesh density increased, value of maximum stress also increased. With a mesh of 82,998 elements, no further increase in maximum stress was observed. The maximum stress value increased by 11 times its initial value as the mesh density increased – aligning with previous findings on mesh convergency reported by Halliday (2023).

For the mapped mesh in Patran, the maximum stress value was 665 MPa for 5,510 elements, increasing to 787 MPa as the number of elements increased to 7,481. A 17.8% increase in stress value was observed with increasing mesh density. Mesh convergence was achieved with a fairly small increment in mapped mesh density – a finding also noted by Jalammanavar et al. (2018).

In Ansys, the maximum stress was 494 MPa for a free mesh of 2,731 elements. As the mesh density increased, the maximum stress value also increased. With a mesh of 72,321 elements, no further increase in maximum stress was observed. Note that the maximum stress value increased by 37.4% of its initial value with increasing mesh density. For the mapped mesh, the maximum stress was 739 MPa for 5,400 elements, increasing to 782 MPa as the number of elements increased to 7294. Here only a 6% increase in stress value was observed with increasing mesh density.

This 6% increase observed in our study contradicts with Svetlichny's (2022) prediction of an increase of 24% in maximum stress. This discrepancy can likely be attributed to differences in the modeling approach. Svetlichny's model incorporated such factors as different boundary conditions and material properties, which may account for the higher stress increase. Further investigation into these differences in maximum value of stress with different boundary conditions and material properties could be a fruitful avenue of new research in this field.

A significant increase in maximum stress was observed with larger density of the free mesh in Patran. This is likely because Patran does not provide control over the local mesh density in regions of geometrical transition and stress gradients, resulting in underpredicted stress values due to discretization errors arising from a coarse mesh. In the case of free mesh in Ansys, in contrast, the increase in maximum stress is not as high as for Patran, likely because of the local mesh refinement in the areas of geometric transition and stress gradients.

For the mapped meshes, the increase in maximum stress value was not large at higher mesh density. Static structural analysis of the model yielded Factor of Safety (FOS) calculations ranging from 1.06 to 1.38 across the different mesh models

Conclusion

This study addressed a critical research question in numerical simulations: whether free and mapped meshes provide consistent results for grid-independent solutions. The

expectation was that as the mesh refines, the solution should converge to a consistent value, reflecting insensitivity to the mesh. The study added further complexity to this by comparing free and mapped meshes across two prominent FEA software platforms, Ansys and Patran.

Contrary to the initial hypothesis, the results revealed that free and mapped meshes do not yield identical results, even with proper mesh convergence. Mapped meshes demonstrated superior accuracy over free meshes, highlighting the significant impact the choice of mesh type can have on simulation accuracy.

Equivalent 3D solid elements in Patran and Ansys, used for static structural analysis, showed consistent results in identifying maximum deformation and stress locations in free and mapped mesh models. However, during free mesh convergence studies in both software platforms, there was a notable increase in maximum stress with successive refinement, indicating sensitivity to mesh density – especially in Patran. Ansys exhibited a smaller increase compared to Patran, demonstrating better stability.

Mapped meshes proved to be more efficient, requiring fewer elements than free meshes for numerical approximation, and the solution becomes mesh-independent at a coarser level. In both Patran and Ansys, maximum stress was higher in mapped meshes than in free meshes. Notably, both software platforms provided the same maximum stress value for the mapped meshes, resulting in consistent Factors of Safety (FOS).

This emphasizes the need for a detailed exploration and understanding of the specific problem at hand when selecting a mesh type. Mapped meshes, with their structured nature, prove advantageous in regular geometries, enhancing efficiency and accuracy. Conversely, free meshes provide flexibility for irregular geometries but demand finer resolutions. Integrating machine learning techniques into automated mesh generation algorithms could optimize mesh quality.

The performance of different mesh types may be sensitive to simulation parameters and specific solver settings, potentially influencing observed results. The observed superiority of mapped meshes may be specific to certain simulations or physical phenomena. Additionally, mapped meshes may entail higher computational costs in terms of mesh generation and simulation time. Evaluating and balancing the trade-off between accuracy and computational efficiency is crucial in this context.

For greater robustness, additional validation against experimental data or benchmark cases is recommended to ensure result reliability. As FEA software continues to improve, particularly in generating similar outcomes for both free and mapped meshes, the conclusions of this study may evolve.

Future research should investigate the underlying reasons for the observed differences in convergence rates and computational efficiency. Understanding the conditions under which mapped meshes outperform free meshes, and examining the impact of element shapes and connectivity on solution accuracy, would provide valuable insights for meshing strategies.

Extending this study's application to interdisciplinary fields, such as fluid-structure interaction, heat transfer, and electromagnetics, could help verify whether the observed trends are consistent across diverse physical phenomena. Exploring hybrid meshing strategies, combining the strengths of free and mapped meshes, could be a promising direction for advancing FEA practices.

References

Arndt, D., Bangerth, W., & Davydov, D. (2021). Finite element library: Design, features, and insights. *Computers & Mathematics with Applications, 81*, 407-422. https://doi.org/10.1016/j.camwa.2020.02.022

De Mooij, C., Martinez, M., & Benedictus, R. (2019). iFEM benchmark problems for solid elements. *Smart Materials and Structures, 28*(6), 065003. https://doi.org/10.1088/1361-665X/ab136f

Ereiz, S., Duvnjak, I., & Jiménez-Alonso, J. F. (2022). Review of finite element model updating methods for structural applications. *Structures*, *41*, 684-723. https://doi.org/10.1016/j.istruc.2022.05.041

Halliday, A., Vulpe, C., & Fourie, A. (2023). A comparison of finite element software for use in tailings applications. In *91st Annual ICOLD Meeting*, ICOLD.

Hoppe, H. (2023). Progressive meshes. In *Seminal Graphics Papers: Pushing the Boundaries, 2*, 111-120. https://doi.org/10.1145/3596711.3596725

İrsel, G. (2019). The effect of using shell and solid models in structural stress analysis. *Vibroengineering PROCEDIA, 27*, 115-120. https://doi.org/10.21595/vp.2019.20977

Jalammanavar, K., Pujar, N., & Raj, R. V. (2018). Finite element study on mesh discretization error estimation. *2018 International Conference on Computational Techniques, Electronics and Mechanical Systems (CTEMS)*, 344-350. https://doi.org/10.1109/CTEMS.2018.8769258

Jiang, Z., Zhang, Z., & Hu, Y. (2021). Bijective and coarse high-order tetrahedral meshes. *ACM Transactions on Graphics (TOG), 40*(4), 1-16. https://doi.org/10.1145/3450626.3459840

Kurowski, P. M. (2022). *Finite element analysis for design engineers*. Pennsylvania: SAE International.

Liu, Z., Chen, J., & Xia, Y. (2021). Automatic sizing functions for unstructured mesh generation. *Engineering Computations, 38*(10), 3995-4023. https://doi.org/10.1108/EC-12-2020-0700

Magomedov, I., & Sebaeva, Z. (2020). Comparative study of finite element analysis software packages. *Journal of Physics: Conference Series*, *1515*(2020), 032073. https://doi.org/10.1088/1742-6596/1515/3/032073

Marcé-Nogué, J., Fortuny, J., Gil, L., & Sánchez, M. (2020). On improving mesh generation in finite element analysis. *Spanish Journal of Palaeontology, 30*(1), 117-132. https://doi.org/10.7203/sjp.30.1.17227

Nemade, A., & Shikalgar, A. (2020). The mesh quality significance in finite element analysis. *IOSR Journal of Mechanical and Civil Engineering (IOSR-JMCE), 17(2)*, 44-48. https://doi.org/10.9790/1684-1702054448

Okereke, M., & Keates, S. (2018). Finite element mesh generation. In *Finite element applications: A practical guide to FEM process* (p. 165-186). https://doi.org/10.1007/978-3-319-67125-3_6

Papadimitrakis, D., Armstrong, C. G., & Robinson, T. T. (2022). Investigating singularities in hex meshing. In *Mesh generation and adaptation: Cutting-edge techniques* (p. 41-67). https://doi.org/10.1007/978-3-030-92540-6_3.

Park, M., Kleb, W., Jones, W., Krakos, J., Todd, M., Loseille, A., Haimes, R., & Dannenhoffer, J. (2019). Geometry modeling for unstructured mesh adaptation. *AIAA Aviation 2019 Forum*. https://doi.org/10.2514/6.2019-2946.

Pietroni, N., Campen, M., Sheffer, A., Cherchi, G., Bommes, D., Gao, X., Scateni, R., Ledoux, F., Remacle, J. & Livesu, M. (2022). Hex-mesh generation and processing: A survey. *ACM Transactions on Graphics, 42*(2), 1-44.

Ruggiero, A., D'Amato, R., & Affatato, S. (2019). Comparison of meshing strategies in finite element modelling. *Materials, 12*(14), 2332. https://doi.org/10.3390/ma12142332

Sabat, L., & Kundu, C. K. (2020). History of Finite Element Method: A Review. In *Recent Developments in Sustainable Infrastructure* (pp. 395–404). Springer Singapore. https://doi.org/10.1007/978-981-15-4577-1_32

Schröder, J., Wick, T., & Reese, S. (2021). A selection of benchmark problems in solid mechanics and applied mathematics. *Archives of Computational Methods in Engineering, 28*(2), 713-751. https://doi.org/10.1007/s11831-020-09477-3

Shah, M., Yunus, M., & Rani, M. (2022). A comparison of FE modelling techniques of composite structure using MSC Patran/Nastran and Ansys software. *AIP Conference Proceedings, 2545*(1), 7. https://doi.org/10.1063/5.0103287

Sher, R. J., Irfan-ul-Hassan, M., & Ghafoor, M. T. (2020). Analysis and design of box girder and t-beam bridge superstructure; A comparative study. *Mehran University Research Journal of Engineering & Technology, 39*(3), 453-465. https://doi.org/10.22581/muet1982.2003.01

Smitha, T. (2021). A study on various mesh generation techniques used for engineering applications. *Journal of Innovative Image Processing, 3*(2), 75-84. https://doi.org/10.36548/jiip.2021.2.001

Svetlichny, J. (2022). Overview of Ansys meshing pre-processor capabilities to create high quality meshes. *Open Information and Computer Integrated Technologies, 5*(95), 83-113. https://doi.org/10.32620/oikit.2022.95.07